Deactivation effects of the lowest excited states of Er^{3+} and Ho^{3+} introduced by Nd^{3+} ions in $LiYF_4$ crystals

F. H. Jagosich, L. Gomes,[a] L. V. G. Tarelho, L. C. Courrol, and I. M. Ranieri
Instituto de Pesquisas Energéticas e Nucleares-Centro de Lasers e Aplicações, Caixa Postal 11049, CEP 05422-970, São Paulo, SP, Brazil

(Received 17 November 2000; accepted for publication 28 September 2001)

The deactivation effects of the lowest excited states of Er^{3+} and Ho^{3+} introduced in Er-or Ho-$LiYF_4$ (YLF) crystals, codoped with Nd ions, were observed by the activator's fluorescence decays. In the case of Er:Nd:YLF, the $^4I_{13/2}\rightarrow{}^4I_{15/2}$ and $^4I_{11/2}\rightarrow{}^4I_{13/2}$ transitions at 1.5 and 2.7 μm, respectively, were analyzed. The $^5I_7\rightarrow{}^5I_8$ and $^5I_6\rightarrow{}^5I_7$ transitions at 2.1 and 2.9 μm, respectively, were investigated for the Ho:Nd:YLF system. Laser excitations generated by a tunable optical parametric oscillator were used in this investigation. The use of a resonant laser excitation to induce the fluorescence allowed accurate measurements of the donor fluorescence decay by a time-resolved infrared spectroscopic system with a time resolution of 0.5 μs. As a result, a general criterion for the migration mechanism, involved in the donor to acceptor energy transfer, was proposed and depends on a parameter $\boldsymbol{R}$. This parameter was defined as the ratio between the transfer rate obtained from the best fit of the fluorescence decay and the theoretical transfer rate predicted by the diffusion model. It was observed that the donor to acceptor transfer is always dominated by a diffusion migration ($\boldsymbol{R}\sim1$) if the donor is in the second excited state, despite a great variation of the C_{DD}/C_{DA} ratio (from ~1 to 371). Nevertheless, a discrete energy migration was found to dominate in the [Ho, Er]→Nd energy transfer when the first excited state of the activator is involved. In this case, the experimental value of the transfer rate is smaller than expected according to the hopping model. Introducing a finite trapping efficiency of an exciton migration in the hopping model, all the observed experimental results were explained. The presence of Nd ions, in addition to decreasing the lifetime of the first excited state of Er^{3+} and Ho^{3+} in YLF, also depopulates the second excited state (partially), depending on the Nd concentration used. © *2002 American Institute of Physics.* [DOI: 10.1063/1.1421208]

I. INTRODUCTION

There is a continuous interest in the improvement of erbium (or holmium) $LiYF_4$ (YLF) laser efficiencies near 3 μm concerning the enhancement of the pumping frequency to values greater that 15 Hz. The upper limit of the operation frequency expected for the 2.7 μm erbium laser (Er:YLF) is intrinsically limited by the longest lifetime of the lower-laser level in comparison with the lifetime of the upper-laser level. The lifetime of the $^4I_{13/2}$ of Er^{3+} is three times longer than that observed for the $^4I_{11/2}$ state. In the case of Ho^{3+}, the lower-laser level ($^5I_7$) is five times longer than that observed for the upper-laser level ($^5I_6$). This intrinsic emission properties of Er (or Ho):YLF allows a self-terminated laser emission (at ~3 μm) with the increase of the pumping frequency. This effect justifies the investigation of the deactivation effect caused in the first excited state of Ho^{3+} (or Er^{3+}) by Nd^{3+} ions in YLF crystals codoped with Nd. These laser systems are very promising for the development of the 3 μm infrared lasers for medical and dentistry applications.[1–4]

Our preliminary work has demonstrated that Nd^{3+} ions can be used to deactivate the first excited state of Er^{3+} and Ho^{3+} at the expense of some depopulation of the upper laser level in YLF.[5] It was concluded that Nd^{3+} introduces the smallest depopulation of the upper laser level, in comparison with the effects introduced by Tb^{3+} and Eu^{3+}. Encouraged by this result, we began to investigate the effect caused in Er^{3+} and Ho^{3+} fluorescence by the presence of Nd ions. A discussion of the differences encountered in the deactivation mechanisms of the lower and the upper laser levels of Er^{3+} and Ho^{3+} as a function of the Er (or Ho) and Nd concentrations was done in this article. Figure 1 shows a schematic energy level diagram representing the (Ho–Nd) and (Er–Nd) interacting systems in the YLF crystal. Holmium and erbium will be designed as activator (or donors) because they are responsible for the laser emission, while the ion responsible for the depopulation of the activator levels will be called deactivator or acceptors—that is the role of Nd ions in this article. In this figure, it is indicated that all the nonradiative pathways were involved in Ho→Nd and Er→Nd energy transfer. In the energy transfer from Ho($^5I_7$)→Nd($^4I_{13/2}$) occurs an emission of two or three phonons by the donor, due to the existence of an energy mismatch between the electronic transitions involved. On the other hand, the Er($^4I_{13/2}$)→Nd($^4I_{15/2}$) energy transfer is resonant.

To investigate the mechanism of migration involved in these energy transfers, the experimental transfer rates K (obtained from best fitting of the donor luminescence decay) were compared to the theoretical transfer rates predicted for

[a]Author to whom correspondence should be addressed; electronic mail: lgomes@net.ipen.br

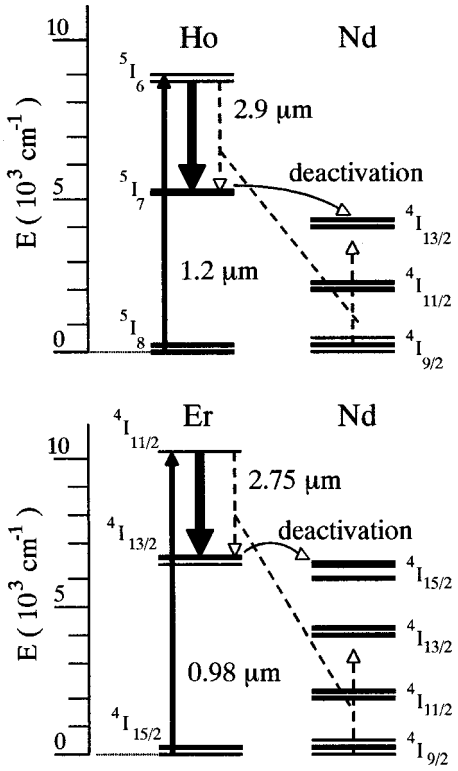

FIG. 1. Schematic diagram of the energy levels of Ho^{3+}, Er^{3+}, and Nd^{3+} ions in YLF showing the nonradiative processes involving the energy transfers to Nd^{3+}. Solid arrow indicates the deactivation process of the first excited state of the activator and dashed line indicates the energy transfer from the second excited state of the activator to Nd^{3+}.

donor $(D) \rightarrow$acceptor(A) transfer assisted either by diffusion or hopping migration. The fitting parameters can be obtained using the Yokota–Tanimoto and Burshtein expressions[6,7] to fit the decay curve of donor luminescence. It was observed that all the energy transfers involved in Er→Nd and Ho→Nd systems have the assistance of the donor migration.

The methodology proposed in this article, to determine the true migration mechanism involved in the $D \rightarrow A$ energy transfer, is general and can be applied to any other crystal. This method allows the determination of the best combination between the activator and deactivator concentrations to minimize (or to avoid) the bottleneck effect existing in this four level system produced by the longer lifetime of the lower laser level (~12 ms) in comparison with the upper level (~4 ms). Furthermore, the proposed model extends the applicability of the hopping migration model for many others systems having larger value of C_{DD}/C_{DA} ratio (from 1 to 701). With this model, it was possible to predict the total lifetime of the upper and the lower laser level as a function of the activator and deactivator concentrations.

II. EXPERIMENTAL PROCEDURE

The samples used in this work were single- and double-doped crystals. Single-doped crystals were: Ho(0.7%):YLF, Er(1%):YLF, and Nd(1.2%):YLF. Double-doped crystals were: Er(1.7%):Nd(1.2%):YLF and Ho(1.5%):Nd(1.2%):YLF. All samples were properly oriented with the c axis placed in a plane perpendicular to sample thickness (or optical length) in the vertical position. Laser excitations were done perpendicular to the sample thickness and the luminescence was observed to be perpendicularly to the excitations. The geometry used in the experiments allowed the absorption and luminescence measurements of the optical transitions having equal distribution of σ and π polarization contributions (without the polarization effect). The lifetimes of excited Ho^{3+} and Er^{3+} were measured using a pulsed laser excitation (4 ns) from a tunable optical parametric oscillator pumped by the second harmonic of a Q-switched Nd-YAG laser from Quantel. Laser excitations at 0.98 and 1.5 μm were used to excite the $^4I_{11/2}$ and $^4I_{13/2}$ states of Er^{3+}, respectively, and laser excitations at 1.15 and 1.95 μm were used to excite the $^5I_6$ and $^5I_7$ states of Ho^{3+}, respectively.

The time-dependent luminescence of the activator was detected by a InSb (77 K) infrared detector (Judson model J10D) with a fast preamplifier (response time of 0.5 μs) and analyzed using a signal-processing box-car averager (PAR 4402).

III. RESULTS

A. Determination of the energy transfer microparameters

The microparameters (C_{DD} and C_{DA}) involved in the energy transfer from the first and the second excited states of the donors (or activators) to the acceptor (or deactivators) were calculated using

$$C_{DD}=\frac{R_{DD}^6}{\tau_0},$$

$$C_{DA}=\frac{R_{DA}^6}{\tau_0},$$

where τ_0 is the total lifetime of the donor state without the presence of the acceptor. The critical radius R_{DD} and R_{DA} were calculated using the overlap integral method based on the calculation of the emission (donor) and the absorption (acceptor) cross-section superposition. The extended overlap-integral method[8] was used to calculate R_{DA} in the case of a nonresonant (or phonon-assisted) energy transfer. The following expressions were used:

resonant

$$R_{DD}^6=\frac{6c\tau_0}{(2\pi)^4 n^2}\frac{g_D^{low}}{g_D^{up}}\int \sigma_{emis}^D(\lambda)\sigma_{abs}^D(\lambda)d\lambda$$

phonon-assisted

$$R_{DA}^6=\frac{6c\tau_0}{(2\pi)^4 n^2}\frac{g_D^{low}}{g_D^{up}}\sum_{N=0}^{\infty}\int \sigma_{emis}^D(\lambda_N^+)\sigma_{abs}^A(\lambda)d\lambda \times\left(\sum_{k=0}^{N} P_{(N-k)}^+ P_k^- P_k^+\right),$$

where N is the total number of phonons involved in the process, $(N-k)$ is the number of phonons emitted (or created) by the donor, and k is the number of phonons absorbed (or

TABLE I. The microparameters calculated for the nonradiative energy transfer from the first and second excited state of Ho^{3+} and Er^{3+} to Nd^{3+} ions in YLF crystal. C_{DD} and C_{DA} constants were obtained by using the method of the extended overlap integral for resonant and nonresonant energy transfers.

$(D\rightarrow A)$ Energy transfer	N(#) (% phonons)	C_{DA} (cm^6/s)	C_{DD} (cm^6/s)	R_{DA} (Å)
Microparameters of deactivation of the first excited states of Ho^{3+} and Er^{3+}				
$Ho(^5I_7)\rightarrow$ $Nd(^4I_{13/2})$	2, 3 (58%, 42%)	$(8.3\pm1.2)\times10^{-41}$	$(5.8\pm0.9)\times10^{-38}$	10.4
$Er(^4I_{13/2})\rightarrow$ $Nd(^4I_{15/2})$	0, 1 (73%, 27%)	$(1.5\pm0.2)\times10^{-40}$	$(4.1\pm0.6)\times10^{-39}$	10.9
Microparameters of deactivation of second excited state of Ho^{3+} and Er^{3+}				
$Ho(^5I_6)\rightarrow$ $Nd(^4I_{13/2})$	2 (100%)	$(4.7\pm0.7)\times10^{-42}$	$(1.7\pm0.3)\times10^{-39}$	4.9
$Er(^4I_{11/2})\rightarrow$ $Nd(^4I_{13/2})$	1 (100%)	$(1.3\pm0.2)\times10^{-40}$	$(2.4\pm0.4)\times10^{-40}$	9.0

annihilated) by the acceptor. λ_N^+ denotes the wavelength translation of the emission cross-section spectrum by $E=[N\hbar\omega]^{-1}$, due to the multiphonon emission by the donor. $P_{(N-k)}^+$ is the probability of multiphonon emission by the donor state. P_k^- is the probability of the acceptor to absorb k phonons and P_k^+ is the probability of the acceptor to emit k phonons in the process. The electron–phonon coupling constant S_0 has been estimated to be ~0.31 and the mean-phonon energy that couples with the phonon sideband is $\hbar\omega\sim331\,cm^{-1}$ for Er^{3+} and Ho^{3+} in YLF crystals.[9] Table I shows the microscopic parameters obtained from this calculation.

Figure 2(a) shows the spectral cross-section superposition between the $^4I_{13/2}\rightarrow{}^4I_{15/2}$ emission band of Er^{3+} (solid line) and the fundamental absorption band of $^4I_{9/2}\rightarrow{}^4I_{15/2}$ transition of Nd^{3+}. Figure 2(b) shows the spectral cross-section superposition between the $^5I_7\rightarrow{}^5I_8$ emission band of Ho^{3+} (solid line) and the $^4I_{9/2}\rightarrow{}^4I_{13/2}$ fundamental absorption of Nd^{3+} due to a nonresonant energy transfer involving two (58%) and three (42%) phonons emission by the donor. Figure 3(a) exhibits the spectral cross-section overlaps between the $^4I_{11/2}\rightarrow{}^4I_{13/2}$ emission band of Er^{3+} (solid line) and the $^4I_{9/2}\rightarrow{}^4I_{13/2}$ fundamental absorption of Nd^{3+} involving one and two phonons absorption by Er^{3+}. Figure 3(b) shows the spectral cross-section superposition between the $^5I_6\rightarrow{}^5I_7$ emission band of Ho^{3+} (solid line) and the $^4I_{9/2}\rightarrow{}^4I_{13/2}$ fundamental absorption of Nd^{3+}, due to two phonons absorption by Ho^{3+}.

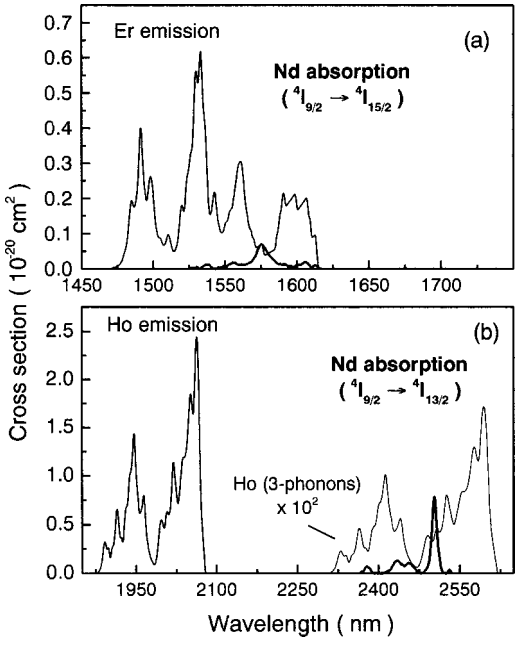

FIG. 2. (a) The spectral cross-section superposition between the $^4I_{13/2}\rightarrow{}^4I_{15/2}$ emission of Er^{3+} at 1.55 μm (solid line) and the fundamental absorption of Nd^{3+} ($^4I_{9/2}\rightarrow{}^4I_{15/2}$). (b) The overlap between the $^5I_7\rightarrow{}^5I_8$ emission of Ho^{3+} at 2 μm (solid line) and the $^4I_{9/2}\rightarrow{}^4I_{13/2}$ fundamental absorption of Nd^{3+} (dark solid line).

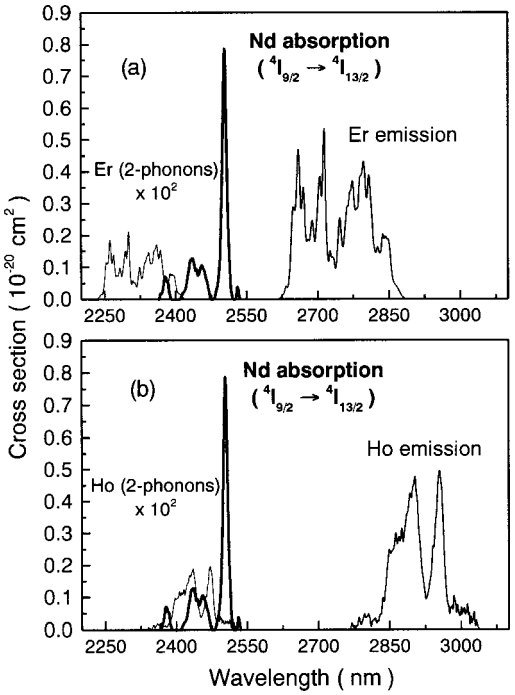

FIG. 3. (a) The spectral cross-section superposition between the $^4I_{11/2}\rightarrow{}^4I_{13/2}$ emission sideband (two-phonon absorption) of Er^{3+} at ~2.4 μm (solid line) and the absorption $^4I_{9/2}\rightarrow{}^4I_{13/2}$ of Nd^{3+} (dark solid line). (b) The overlap of $^5I_6\rightarrow{}^5I_7$ emission sideband (two-phonon absorption) of Ho^{3+} at 2.5 μm (solid line) and the $^4I_{9/2}\rightarrow{}^4I_{13/2}$ absorption of Nd^{3+} (dark solid line). The emission bands of Er^{3+} at 2.7 μm and of Ho^{3+} at 2.9 μm were also exhibited.

B. Analysis of the donor fluorescence decay

Donor fluorescence decay in the presence of the acceptor was analyzed using current models found in the literature, which consider the excitation migration between donors. For many materials with high enough activator concentration ($\geqslant$1 mol %), one verifies that the excitation energy can be transferred from one activator to another several times before the occurrence of the final transfer to an acceptor. In this kind of multistep transfer process, the excitation energy can be described as a quasiparticle migrating on a lattice of activators, and the mathematical description of the process is the same as the one used for the exciton migration. This case

involves a localized exciton with electron and hole, both located on the same ion and moving together as a Frenkel exciton.[10]

The dynamic of the total energy transfer process is characterized by two distinct contributions: the migration of energy among activator ions and the energy trapping at deactivator sites. When the donor migration can be treated like the exciton diffusion model, one can use the multistep random walk model to solve the $D \rightarrow A$ energy transfer problem and find the transfer rate term associated with the donor migration. If a large number of diffusion steps can be done before the excitation can be trapped by the acceptor and then become extinct, one can obtain the time dependence of activator fluorescence by solving the diffusion equation of the system.[10] No general solution to this equation has been obtained. However, the $D \rightarrow A$ energy transfer rate K_d involving diffusion can be calculated from the multistep energy transfer, treating the diffusion between donors like a random walk. In this model it is assumed that any excitation created at time $t=0$, within the trapping radius R_T, has an infinite trapping rate.[10] Any diffusing excitation by an electric dipole–dipole interaction between donors on a cubic lattice has a trapping radius defined as the distance at which the $D \rightarrow A$ transfer rate is equal to the rate of $D \rightarrow D$ transfer. This gives $R_T = 0.676(C_{\mathrm{DA}}/D)^{1/4}$. The diffusion coefficient (cm^2/s) is given by $D = \frac{1}{2}(4\pi c_D/3)^{4/3}\ C_{\mathrm{DD}}$ and the energy transfer rate, which is associated with diffusion and trapping derived from the random walk treatment, is given by $K_d = 4\pi D R_T c_A$. This can be related to the microscopic parameters of the interaction by

$$K_d = 21\ \ c_A\ \ c_D(C_{\mathrm{DD}}^3\ \ C_{\mathrm{DA}})^{1/4}. \tag{1}$$

In this equation, c_D and c_A are the donor and acceptor concentrations in cm^{-3} and C_{DD} (or C_{DA}) is given in cm^6/s.

Yokota–Tanimoto[6] have obtained a solution of the donor fluorescence decay for the limited case of a weak diffusion perturbing a strong donor–acceptor interaction, which is given by

$$I(t) = I_0 \exp\left(-\frac{t}{\tau_0} - \gamma\sqrt{t}\left(\frac{1+10.87y+15.5y^2}{1+8.743y}\right)^{3/4}\right),$$

$$y = D\frac{\tau_0}{R_{\mathrm{DA}}^2}\left(\frac{t}{\tau_0}\right)^{2/3},$$

$$D = \frac{1}{2}\left(\frac{4\pi c_A}{3}\right)^{4/3} C_{\mathrm{DD}}$$

$$\gamma = \frac{4\pi^{3/2}}{3} c_A R_{\mathrm{DA}}^3 \frac{1}{\sqrt{\tau_0}},$$

where γ and y are the fitting parameters. One should note that $\gamma(\mathrm{s}^{-1/2})$ is the transfer parameter without excitation migration and that the transfer rate K involving diffusion is indirectly obtained from y and D.

Another approach is the hopping model, which can be applied to describe the incoherent excitation migration between donor states using the average hopping time t_h, i.e., the excitation will be scattered at each step in the random walk. If a trapping radius is defined as the distance at which the rate of donor–acceptor transfer is equal to the hopping rate, the overall energy transfer rate becomes[11]

$$K_h = 20 c_A c_D (C_{\mathrm{DD}} C_{\mathrm{DA}})^{1/2}. \tag{2}$$

Burshtein[7] has obtained a solution for the donor fluorescence decay when the energy transfer involves the excitation migration through donor states in a stochastic hopping process (valid for the cases where $C_{\mathrm{DD}} > C_{\mathrm{DA}}$). This solution is given by

$$I(t) = I_0 \exp(-t/\tau_0 - \gamma\sqrt{t} - Kt),$$

where $\gamma(\mathrm{s}^{-1/2})$ and $K(\mathrm{s}^{-1})$ are the fitting parameters.

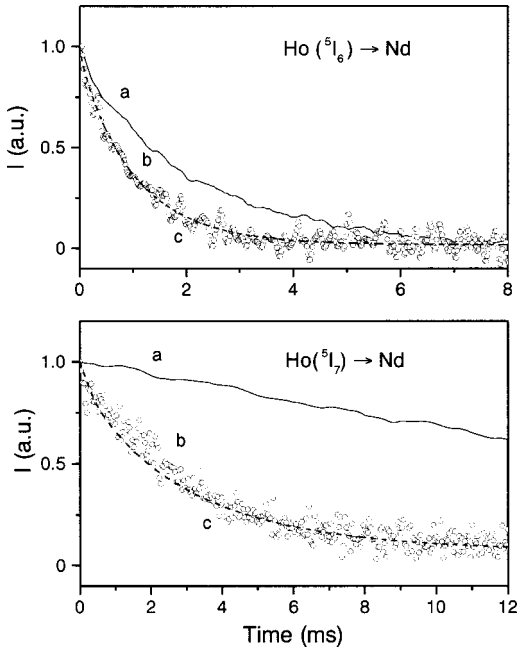

FIG. 4. The fluorescence decay of Ho^{3+} at 2.9 and 2.1 μm from the $^5I_6$ and $^5I_7$ states, respectively, in YLF crystal at 300 K. This fluorescence was, respectively, excited by a laser pulse of 10 mJ at 1.15 and 1.95 μm. Curve (a) was used for Ho(0.7%):YLF and curve (b) for Ho(1.5%):Nd(1.2%):YLF crystal. Curve (c) was obtained from the best fits of the fluorescence decay of Ho($^5I_6$,$^5I_7$) in the presence of Nd^{3+} ions, using the Burshtein model (dashed line).

Figure 4 shows the fluorescence decay curves of the $^5I_6$ and $^5I_7$ states of Ho^{3+} in Ho:YLF and in Ho:Nd:YLF crystals. Figure 5 shows the fluorescence decay curves of the $^4I_{11/2}$ and $^4I_{13/2}$ states of Er^{3+} in Er:YLF and in Er:Nd:YLF. All these fluorescence measurements were done at 300 K. In both Figs. 4 and 5, curve (a) represents the decay of donor fluorescence without the presence of Nd, curve (b) represents the decay of donor fluorescence modified by the presence of Nd, and curve (c) represents the best fitting of the fluorescence decay. It was observed that the fluorescence decay of donor states of Ho^{3+} and Er^{3+} in single doped YLF are exponentials with a time constant τ_0. The measured values of τ_0 were: 2 ms ($^5I_6$); 20 ms ($^5I_7$); 3.9 ms ($^4I_{11/2}$), and 12 ms ($^4I_{13/2}$). These values are fairly close to the total lifetime found in the literature for these excited states given as 3.1, 15.2, 3.9, and 11 ms, respectively.[12]

The best fittings of the fluorescence decay of donor states were performed using the Burshtein model because the mathematical expression is very simple and the fitted param-

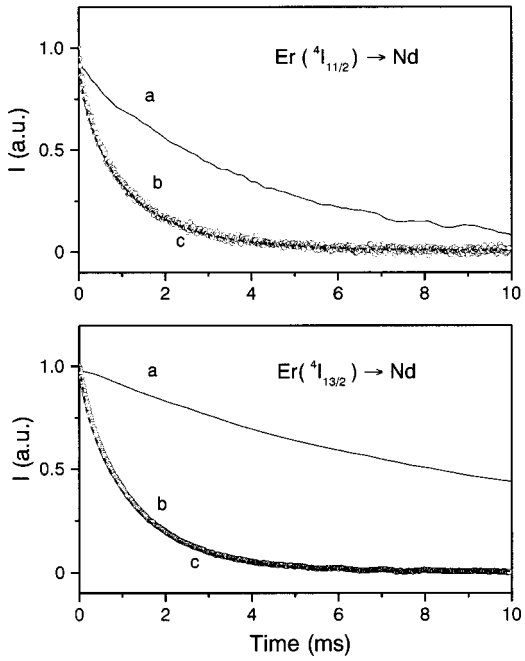

FIG. 5. The fluorescence decay of $^4I_{11/2}$ and $^4I_{13/2}$ state of Er^{3+}, respectively, at 2.75 and 1.6 μm in YLF crystal at 300 K. This fluorescence was excited by a laser pulse of 10 mJ at 0.98 and 1.5 μm, respectively. Curve (a) was obtained for the Er(1%):YLF and curve (b) for Er(1.7%):Nd(1.2%):YLF crystal. Curve (c) was obtained from the best fits of fluorescence decay of Er^{3+} in Er:Nd:YLF crystal, using the Burshtein model (dashed line).

eter K is the transfer rate of the system, i.e., $K \rightarrow K(\text{exp})$. It is always very useful to compare the fit parameter K [or $K(\text{exp})$] with the theoretical values calculated using Eqs. (1) and (2) expected for a donor–acceptor transfer assisted by diffusion K_d and hopping migration K_h, respectively. Table II shows the values of the transfer parameters γ and K obtained from the best fittings of the donor fluorescence decay using the Burshtein expression. Table II also gives the transfer constant K obtained from the Yokota–Tanimoto expression, calculated using the parameter y and the diffusion constant $D(\text{cm}^2/\text{s})$.

The analysis of the donor fluorescence decay showed that the Er (or Ho)→Nd energy transfer is always assisted by donor migration. Because of this fact, the fluorescence decay of the donor could not be fit by the Inokuti–Hirayama solution,[13] which is used for the energy transfer without excitation migration. The challenge of this investigation is to find a way to determine the real mechanism of migration involved in each energy-transfer process: diffusion or hopping migration? In principle, one can always use the Yokota–Tanimoto or Burshtein expressions to fit the donor fluorescence decay for an energy transfer assisted by donor migration, although, best fits can always be performed and the comparison among the best results does not constitute an appropriated way to indicate the real migration mechanism involved in the donor–acceptor energy transfer. In most of the cases, best fittings give similar results making the choice for the real transfer mechanism dubious.

Our analysis of the fluorescence decay of the first excited states of Er^{3+} and Ho^{3+} in the presence of Nd^{3+} ions showed that the energy transfer rate K obtained from the best fit is smaller than the transfer rate K_h predicted by the hopping model. It was observed that $K/K_h \sim 0.77$ for the $\text{Er}(^4I_{13/2}) \rightarrow \text{Nd}$ transfer and $K/K_h \sim 0.14$ in the case of $\text{Ho}(^5I_7) \rightarrow \text{Nd}$. Considering this result, it is clear that the excitation migration through the $^5I_7$ state of Ho^{3+} cannot be described by the current hopping model and that some modification is needed. This modification will be introduced in Sec. IV considering that any migrating exciton must have a finite probability rate of being captured by the acceptor (or to escape from being trapped) when crossing the critical volume centered on the acceptor site. It will be demonstrated that the exciton trapping efficiency is dependent on the $C_{\text{DD}}/C_{\text{DA}}$ ratio. This efficiency is sufficient to correct the theoretical value of K_h (expected by the hopping model) re-

TABLE II. The experimental values of parameters γ and K obtained from best fit using Burshtein and Yokota Tanimoto solutions. Character $\boldsymbol{R}$ is given for a wide survey of energy transfer processes including the systems found in the literature for the YLF crystal. Deviations in the calculated parameters were estimated by error propagation obtained in the absorption and fluorescence measurements.

			Theory overlap		Experimental Burshtein		
$D \rightarrow A$ Energy transfer	$\boldsymbol{R}$ (exp)	$K_d(\text{s}^{-1})$ (theor.)	$C_{\text{DD}}/C_{\text{DA}}$	γ ($\text{s}^{1/2}$)	γ ($\text{s}^{1/2}$)	$K(\text{s}^{-1})$	YT[a] $K(\text{s}^{-1})$
$\text{Ho}(^5I_6) \rightarrow \text{Nd}$	1.8 ± 0.3	300 ± 51	371 ± 85	2.7 ± 0.2	5.5 ± 1.3	532 ± 39	404 ± 30
$\text{Ho}(^5I_7) \rightarrow \text{Nd}$	0.021 ± 0.003	8622 ± 1315	701 ± 149	11.4 ± 0.8	6.6 ± 0.6	186 ± 13	—
$\text{Er}(^4I_{11/2}) \rightarrow \text{Nd}$	1.2 ± 0.2	178 ± 30	1.8 ± 0.4	14.6 ± 1.1	20.2 ± 0.3	218 ± 7	396 ± 13
$\text{Er}(^4I_{13/2}) \rightarrow \text{Nd}$	0.30 ± 0.04	1563 ± 224	27 ± 5	15.4 ± 1.1	10.8 ± 0.2	503 ± 4	354 ± 3
$\text{Tm}(^3H_4) \rightarrow \text{Tb}$	1.66	354	1.4	⋯	⋯	⋯	588[b]
$\text{Tm}(^3F_4) \rightarrow \text{Tb}$	1.50	1188	0.8	⋯	⋯	⋯	1789[b]
$\text{Tm}(^3H_4) \rightarrow \text{Eu}$	0.92	177	5.9	⋯	⋯	163[b]	⋯
$\text{Tm}(^3F_4) \rightarrow \text{Eu}$	0.62	524	5.6	⋯	⋯	324[b]	⋯
$\text{Yb}(^2F_{5/2}) \rightarrow \text{Tm}$	0.36	3250	16.3	⋯	⋯	1267[c]	⋯

[a]YT means Yokota Tanimoto model.
[b]Data were obtained from Ref. 14.
[c]Data obtained from Ref. 15, using the rate equation model.

sulting in an effective transfer rate more compatible with the experimental value obtained for several interacting systems having $(C_{DD}/C_{DA}) \gg 1$.

On the other hand, it was seen that the transfer rate obtained from the best fit of the fluorescence decay of the second excited state of Er^{3+} (or Ho^{3+}) showed values close to the transfer rate K_d predicted by Eq. (1) in the Nd codoped YLF. Nevertheless, the criterion to find the real excitation migration mechanism that governs the donor–acceptor energy transfer is still lacking and it will be introduced in Sec. IV.

IV. DISCUSSION

Let us establish that the character of an energy transfer assisted by donor migration is given by the parameter $\boldsymbol{R}$. This parameter is defined as the ratio between the experimental transfer rate K obtained from the best fit of the donor–fluorescence decay and the transfer rate K_d predicted by the diffusion model

$$\boldsymbol{R} = \frac{K}{K_d}. \tag{3}$$

By definition, $\boldsymbol{R}$ gives the character of the real donor–migration mechanism involved in the energy-transfer process and it is independent of donor and acceptor concentrations. This criterion consists of calculating the character $\boldsymbol{R}$ of an interacting system using $K = K(\text{exp})$ in Eq. (3), and a comparison with the character expected by the energy transfer assisted by diffusion $(R = 1)$ or hopping migration $(\boldsymbol{R} = K_h/K_d)$. One should note that $\boldsymbol{R} \approx 1$ is consistent with a long mean-free-path type of random walk or diffusion model in the energy transfer process. Substituting K_d given by Eq. (1) and K_h [Eq. (2)] in Eq. (3), one gets the character $\boldsymbol{R}_h$ expected for an energy transfer following the current hopping model. $\boldsymbol{R}_h$ is given by

$$\boldsymbol{R}_h = \frac{K_h}{K_d} = \left(\frac{20}{21}\right)\left(\frac{C_{DA}}{C_{DD}}\right)^{1/4}. \tag{4}$$

It is seen that $\boldsymbol{R}_h$ is smaller than unity if $C_{DD} > C_{DA}$.

Several studies of energy transfer have been recently reported in the literature, as Tm $(^3F_4; {}^3H_4) \rightarrow$ Tb,[14] Tm $(^3F_4; {}^3H_4) \rightarrow$ Eu,[14] and Yb$(^2F_{5/2}) \rightarrow$ Tm[15] in YLF crystals, where the migration mechanism is always present. Using the experimental transfer rate $K(\text{exp})$ we calculated the character $\boldsymbol{R}$ for several distinct interacting systems, in order to find the physical relation between $\boldsymbol{R}$ and the C_{DD}/C_{DA} ratio in YLF crystals. Using a great variation of C_{DD}/C_{DA} ratio (from ~0.8 to 701) it was observed that the current hopping migration fails to describe the transfer process with the increase of the C_{DD}/C_{DA} ratio.

The values of $\boldsymbol{R}$ are given in Fig. 6 and were obtained for many interacting systems including the Ho→Nd and Er →Nd investigated in this article and some others calculated from the available transfer constants (C_{DA} and C_{DD}) found in the literature.[14,15] The experimental values of $\boldsymbol{R}$ were obtained using $K = K(\text{exp})$ in Eq. (3) and they were represented by symbols in Fig. 6. The behavior of the first excited state of donor was illustrated by the solid square symbols (open

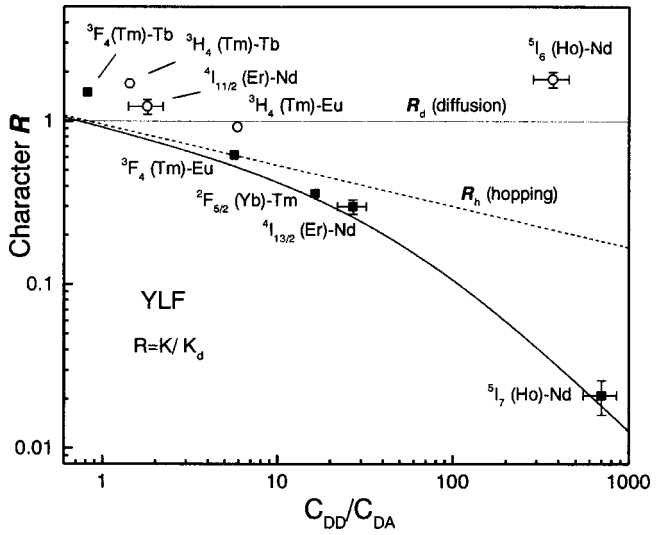

FIG. 6. The calculated character $\boldsymbol{R}$ as a function of $C_{D\text{-}D}/C_{D\text{-}A}$ ratio for an energy transfer assisted by excitation migration using the diffusion model $\boldsymbol{R}_d = 1$ (horizontal solid line) or by the hopping model $\boldsymbol{R}_h$ (dashed line). $\boldsymbol{R}(\text{exp})$ for donors in the first excited state were represented by solid squares and open circles for the second excited state. The characters of Tm$(^3H_4; {}^3F_4) \rightarrow$Tb (Ref. 14), Tm$(^3H_4; {}^3F_4) \rightarrow$Eu (Ref. 14), and Yb$(^2F_{5/2}) \rightarrow$Tm (Ref. 15) transfers were calculated using the transfer constants found in the literature. The solid line shows the predicted behavior of $\boldsymbol{R}(\text{eff})$.

circles were used for the case of the second excited state of donors). The horizontal line $(\boldsymbol{R} = 1)$ exhibited in Fig. 6 represents the behavior of the character $\boldsymbol{R}_d$ expected for any energy transfer assisted by diffusion described by coherent exciton migration (or the diffusion model). On the other hand, the dashed line in Fig. 6 shows the behavior of the character $\boldsymbol{R}_h$ with the increase of the C_{DD}/C_{DA} ratio for many energy transfer systems having a discrete or incoherent exciton migration as currently described by the hopping model. Several important observations can be derived from the experimental results exhibited in Fig. 6. First, it is seen that the second excited state of the donor always transfers its energy to an acceptor involving the excitation migration through donor states as described in the diffusion model. In this case, the observed characters of the energy transfers were independent of the C_{DD}/C_{DA} ratio, as expected. This observation contradicts the statement found in the literature, which states that a discrete (or incoherent) migration mechanism as the excitation hopping, dominates the energy transfer for the cases where $C_{DD} \gg C_{DA}$.[14,16] This statement is true only for the cases where the donor is in the first excited state. In this case, the energy transfer can follow the current hopping migration only for the systems having $(C_{DD}/C_{DA}) \leqslant 5$. By increasing this ratio, the character $\boldsymbol{R}$ decreases and deviates from the theoretical behavior of $\boldsymbol{R}_h$. The Er$(^4I_{13/2}) \rightarrow$Nd and Ho$(^5I_7) \rightarrow$Nd energy transfers showed this unexpected effect.

This observation questions the validity of the assumption used to estimate the transfer rate K_h in the current hopping model: any migrating exciton has an infinite probability rate of being extinct by the acceptor when it crosses the interaction volume. This assumption is true only for cases where $C_{DD} \sim C_{DA}$.

A. Proposed modification in the hopping migration mechanism

We propose that a migrating exciton having a discrete (or incoherent) dipole–dipole interaction with the acceptor must have a finite probability rate of being extinct in the acceptor site. Conversely, this migrating exciton should also have a probability rate of escaping from the extinction when crossing the interaction volume centered in the acceptor. In other words, we affirm that a hopping exciton must have an extinction efficiency given by

$$\eta_T = \frac{W_T}{W_T + W_{nT}}, \tag{5}$$

where W_T is the probability rate (s^{-1}) of exciton trapping and W_{nT} is the probability rate (s^{-1}) of escaping from the acceptor capture. W_T has been given in the current hopping model. However, W_{nT} is now defined as the ratio between the exciton diffusion coefficient D and the area of the closed surface involving the interaction volume centered in the acceptor ion. These two probability rates are given by

$$W_T = \frac{4\pi c_A R_T^3}{3t_h}$$

$$W_{nT} = \frac{D}{4\pi R_T^2}, \tag{6}$$

where R_T is the exciton trapping radius by the acceptor described in the hopping model and t_h is the average hopping time. R_T and t_h are given by[10]

$$R_T = (t_h C_{\mathrm{DA}})^{1/6}$$

$$t_h \cong \frac{27}{8\pi^3}(C_{\mathrm{DD}}\, c_D^2)^{-1}.$$

The diffusion coefficient D described by the random walk problem in a three dimensional lattice is given by[10]

$$D = \frac{1}{6}\frac{\overline{l_h^2}}{t_h}, \tag{7}$$

where l_h is the average step length in the random walk. Using $\overline{l_h^2} \approx (c_D)^{-(2/3)}$ in the expression of D in Eq. (7) and then substituting the result in Eq. (6), one obtains the ratio between these two probability rates given by

$$\frac{W_T}{W_{nT}} = 50\left(\frac{c_A}{c_D}\right)\left(\frac{C_{\mathrm{DA}}}{C_{\mathrm{DD}}}\right)^{5/6}. \tag{8}$$

Using the result of Eq. (8) in Eq. (5), one gets the exciton trapping efficiency η_T. It is convenient to introduce the effective trapping radius and the effective transfer rate in the modified hopping migration given by $\boldsymbol{R}_T(\mathrm{eff}) = \boldsymbol{R}_T \eta_T$ and $K_h(\mathrm{eff}) = K_h \eta_T$, respectively.

The effective character of an energy transfer assisted by the modified hopping model is obtained using $K = K_h(\mathrm{eff})$ in Eq. (3)

$$\boldsymbol{R}_h(\mathrm{eff}) = \boldsymbol{R}_h \frac{1}{1 + 0.02\left(\frac{c_D}{c_A}\right)\left(\frac{C_{\mathrm{DD}}}{C_{\mathrm{DA}}}\right)^{5/6}}. \tag{9}$$

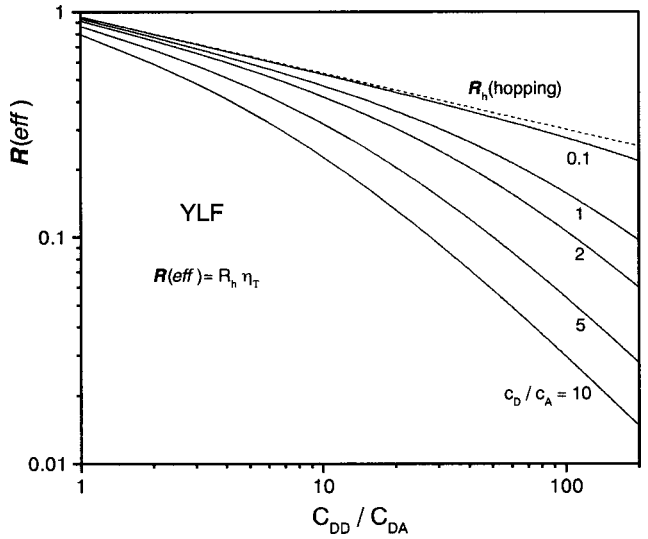

FIG. 7. The behavior of $\boldsymbol{R}$(eff) predicted by Eq. (9), calculated as a function of the $C_{\mathrm{DD}}/C_{\mathrm{DA}}$ ratio for some c_D/c_A concentration ratios (solid line). The dotted line indicates the behavior of $\boldsymbol{R}_h$ predicted using the current hopping model. It is seen that $\boldsymbol{R}$(eff) deviates from $\boldsymbol{R}_h$ with the increase of $C_{\mathrm{DD}}/C_{\mathrm{DA}}$ ratio for a system having $c_D > c_A$.

The obtained values of $\boldsymbol{R}$ for the systems investigated in this work [$\mathrm{Er}(^4I_{13/2}) \rightarrow \mathrm{Nd}$ and $\mathrm{Ho}(^5I_7) \rightarrow \mathrm{Nd}$ transfers] and values of $\boldsymbol{R}$ obtained for the systems encountered in the literature [$\mathrm{Tm}(^3F_4) \rightarrow \mathrm{Eu}$[14] and $\mathrm{Yb}(^4F_{5/2}) \rightarrow \mathrm{Tm}$[15] transfers] are in agreement with the effective character $\boldsymbol{R}_h$(eff) predicted by Eq. (9) as can be seen in Fig. 6 (dark solid line). It is seen that the character $\boldsymbol{R}$ deviates from the behavior of the character $\boldsymbol{R}_h$ of the current hopping model for the systems having $C_{\mathrm{DD}} \gg C_{\mathrm{DA}}$. Nevertheless, the character $\boldsymbol{R}$ in these cases approximates the effective character $\boldsymbol{R}_h$(eff) predicted by the proposed hopping model.

Figure 7 exhibits the behavior of $\boldsymbol{R}_h$(eff) for an energy transfer as a function of $C_{\mathrm{DD}}/C_{\mathrm{DA}}$ ratio using Eq. (9), for some (c_D/c_A) concentration ratios. It is seen in this figure that $\boldsymbol{R}_h$(eff) always decreases with the increase of the $C_{\mathrm{DD}}/C_{\mathrm{DA}}$ ratio, deviating from the expected behavior of the current hopping model $\boldsymbol{R}_h$ (dashed line) for the case where $c_D \geqslant c_A$. Figure 8 shows the probability ratio W_T/W_{nT} as a function of the $C_{\mathrm{DD}}/C_{\mathrm{DA}}$ ratio using $c_D = 2c_A$ in Eq. (8). It can be seen that $W_T \approx W_{nT}$ when $(C_{\mathrm{DD}}/C_{\mathrm{DA}}) = 75$. In this case the exciton trapping efficiency η_T is equal to 0.5. Nevertheless, by the increase of the $C_{\mathrm{DD}}/C_{\mathrm{DA}}$ ratio W_T becomes smaller than W_{nT}, consequently decreasing the exciton trapping efficiency. Therefore, the transfer rate which describes the interacting system must be given by K_h(eff) instead of by K_h.

B. Estimation of the lifetime effects on the upper and the lower laser levels of Ho^{3+} and Er^{3+} by Nd^{3+} ions

Because the knowledge that the energy transfer from the second excited state of the donor is well described by the transfer rate of diffusion model K_d and that the effective transfer rate K_h(eff) well describes the energy transfer from the first excited state of the donor, one can predict the total

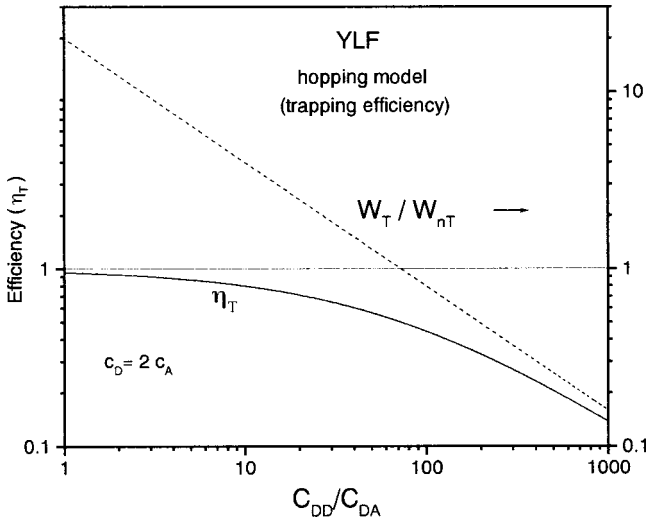

FIG. 8. The theoretical ratio W_T/W_{nT} as function of $C_{\mathrm{DD}}/C_{\mathrm{DA}}$ ratio calculated by Eq. (8) for the case of $c_D=2c_A$. It is seen that W_T is equal to W_{nT} when $C_{\mathrm{DD}}/C_{\mathrm{DA}}$ is 75 given $\eta_T=0.5$ (or 50%).

lifetime of the donor state as a function of donor concentration, if a random donor–donor and donor–acceptor interactions are preserved. The total energy transfer rate from the first excited state of the donor is given by

$$\overline{W}_t(1^{\mathrm{st}})=\gamma^2+\eta_T K_h\,. \tag{10}$$

In the case of the second excited state of the donor, the total energy-transfer rate is given by

$$\overline{W}_t(2^{\mathrm{nd}})\,\gamma^2+K_d\,. \tag{11}$$

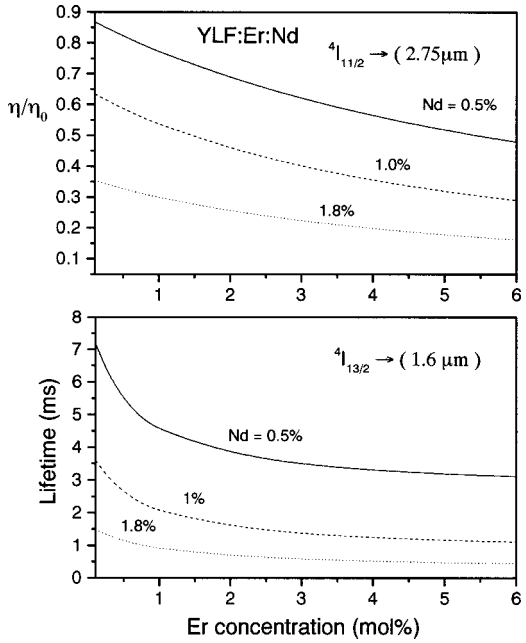

FIG. 9. The relative luminescence efficiency of Er($^4I_{11/2}$) in YLF as function of Er^{3+} concentration for three Nd^{3+} concentrations calculated using Eqs. (13) and (14). The total fluorescence lifetime of Er($^4I_{13/2}$) was calculated using Eqs. (12) and (14) for each system considered. A strong decrease of erbium lifetime for [Nd]>0.5% is shown.

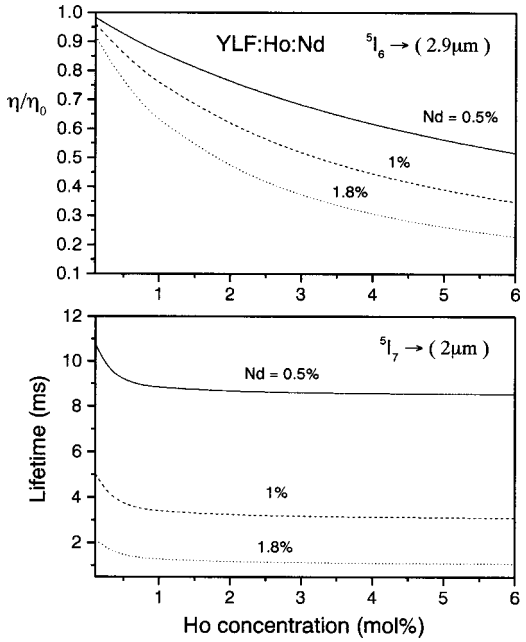

FIG. 10. The relative luminescence efficiency of Ho($^5I_6$) in YLF as a function of Ho^{3+} concentration for three Nd^{3+} concentrations calculated using Eqs. (13) and (14). The total luminescence lifetime of Ho($^5I_7$) was calculated using Eqs. (12) and (14) for each system. A strong decrease of holmium lifetime for [Nd]>0.5% is shown.

The total lifetime τ of a donor state and its relative luminescence efficiency are given by

$$\frac{1}{\tau}=\frac{1}{\tau_0}+\overline{W}_t\,,$$

$$\frac{\eta}{\eta_0}=\frac{\tau}{\tau_0}=1-\tau\overline{W}_t\,, \tag{12}$$

where $\eta_0=\tau_0/\tau_r$ and τ_0 are the luminescence efficiency and the total lifetime of the isolated donor, respectively, τ_r is the radiative lifetime of the donor state, and η is the total luminescence efficiency of the donor state in the presence of the acceptor. Substituting $W_t(1^{\mathrm{st}})$ given by Eq. (10) in Eq. (12), one can estimate the total lifetime of the Er($^4I_{13/2}$) and Ho($^5I_7$) states for several concentrations of Er (or Ho) and Nd. Using $W_t(2^{\mathrm{nd}})$ given by Eq. (11) in Eq. (12), one can also estimate the total luminescence efficiency of the second excited states ($^4I_{11/2}$ and $^5I_6$) of Er^{3+} and Ho^{3+}. Figures 9 and 10 show the calculated effects on the luminescence of Er^{3+} in Er:Nd:YLF and for Ho^{3+} in Ho:Nd:YLF laser crystal, respectively. By observing the predicted lifetime of the lower laser level and the relative luminescence efficiency of the upper laser level of the activator as a function of donor (Er or Ho) and Nd concentrations, one can choose the most convenient concentrations of dopants for the laser medium, which shows a better laser emission performance with the increase in pumping frequency. Nevertheless, the fluorescence analysis of Er^{3+} and Ho^{3+} in Nd codoped YLF crystals employed in this work is suitable for understanding the nonradiative deactivation process of lower laser levels in fluoride laser materials.

V. CONCLUSION

It was demonstrated that the presence of 1.2 mol % of Nd^{3+} ions introduces an effective deactivation process of the lower laser level of Er^{3+} and Ho^{3+} (first excited state) decreasing the lifetime from 10 to 1 ms and from 17 to 2 ms, respectively, in Er:Nd:YLF and Ho:Nd:YLF crystals. Nevertheless, a partial depopulation of the upper laser levels (second excited state) was observed for these systems, which reduces the small signal gain of the laser medium. A criterion was introduced in order to establish the real mechanism of donor–donor migration which helps the donor–acceptor energy transfer, by estimation of the character $\boldsymbol{R}$ of the process. Comparing the character $\boldsymbol{R}$ of the process with the theoretical character expected for the diffusion migration ($\boldsymbol{R}\approx 1$) or with the character expected for the hopping migration, one finds the true migration mechanism involved in each case. It was observed that the second excited state of the activator always followed the diffusion migration despite the great variation of the C_{DD}/C_{DA} ratio of the investigated systems. This result indicates that the second excited state of the donors (Er^{3+}, Ho^{3+}, and Tm^{3+}) always keeps the phase memory of the $D \rightarrow A$ interaction during the excitation migration, similar to what happens in a coherent exciton diffusion. This effect is probably due to the low transition energy involved in these cases (2500–3400 cm^{-1}). However, this phase memory is lost with the transition energy increase, as it occurs with the donor in the first excited state (5300–9700 cm^{-1}). Because of this fact, the excitation migration is discrete, and occurs by the hopping mechanism. However, it was found that the hopping migration, as currently established, well describes only the interacting systems having $C_{DD} \leqslant 5C_{DA}$. For other interacting systems having $C_{DD} \geqslant 10C_{DA}$, the experimental transfer rate K is always smaller than the transfer rate predicted by the current hopping model K_h. The proposed modification in the hopping model, which introduces the exciton trapping efficiency η_T, can describe this transfer rate. Knowing the mechanism of the deactivation of the first excited state (modified hopping migration) and the depopulation of the second excited state (diffusion model) by Nd^{3+} ions in (Ho:Nd) and (Er:Nd):YLF, we estimate the total lifetime of the lower and of the upper laser levels as a function of the activator and the deactivator (Nd) concentrations. With this result, one can evaluate the most convenient concentrations of the activator and neodymium used to compose the laser medium. The depopulation of the upper laser level of the erbium and holmium introduced by neodymium (predictable) limits the use of high concentration of the Er (or Ho) in Nd codoped YLF laser crystal.

ACKNOWLEDGMENTS

The authors would like to express their sincere thanks to Professor Spero Penha Morato of the IPEN, for his critical reading of the manuscript and fruitful discussions. One of the authors, F.H.J. thanks FAPESP for the fellowship. They also thanks FAPESP for financial support of this work (Grant No. 1995/4166-0) and CNPq.

[1] P. Moulton, E. Adamkiewicz, and S. Wright, Laser Focus World, 65 (1992).
[2] J. Hecht, Laser Focus World **Nov.** 135 (1993).
[3] B. Struve and G. Huber, J. Phys. IV **1**, C7-3 (1991).
[4] J. H. Kinney, D. L. Haupt, M. Balloch, J. M. White, W. L. Bell, S. J. Marshall, and G. W. Marshall, J. Dent. Res. **75**, 1388 (1996); H. K. Park and R. F. Haglund, Jr., Proc. SPIE **2973**, 101 (1997).
[5] F. H. Jagosich, L. V. G. Tarelho, L. Gomes, L. C. Courrol, and I. M. Ranieri, paper presented at the International Conference on Defects in Insulating Materials, ICDIM2000, South Africa, 2000.
[6] M. Yokota and O. Tanimoto, J. Phys. Soc. Jpn. **22**, 779 (1967).
[7] A. I. Burshtein, Sov. Phys. JETP **35**, 882 (1972).
[8] L. V. G. Tarelho, L. Gomes, and I. M. Ranieri, Phys. Rev. B **56**, 14344 (1997).
[9] G. M. Renfro, J. C. Windscheif, and W. A. Sibley, J. Lumin. **22**, 51 (1980).
[10] Richard C. Powell, in *Physics of Solid-State Laser Materials*, edited by R. C. Powell (Springer, New York, 1998), Chap. 5.
[11] R. K. Watts, in *Optical Properties of Ions in Solids*, edited by B. DiBartolo (Plenum, New York, 1975), p. 307.
[12] C. Li, Y. Guiot, C. Linares, and R. Moncorgé, OSA Proc. Adv. Solid-State Lasers **15**, 91 (1993).
[13] M. Inokuti and F. Hirayama, J. Chem. Phys. **43**, 1978 (1965).
[14] A. Braud, S. Girard, J. L. Doualan, and R. Moncorgé, IEEE J. Quantum Electron. **34**, 2246 (1998).
[15] Y. Mita, T. Ide, M. Togashi, and H. Yamamoto, J. Appl. Phys. **85**, 4160 (1999).
[16] A. Braud, S. Girard, J. L. Doualan, M. Thuau, and R. Moncorgé, Phys. Rev. B **61**, 5280 (2000).